STATISTICAL MODELLING OF EARTH'S PLASMASPHERE

by

Victoir Veibell

A Dissertation
Submitted to the
Graduate Faculty
of
George Mason University
In Partial fulfillment of
The Requirements for the Degree
of
Doctor of Philosophy
Computational Space Sciences and Astrophysics

Committee:

_____ Robert Weigel, Dissertation Director

_____ Kirk Borne, Committee Member

_____ Fernando Camelli, Committee Member

_____ Jie Zhang, Committee Member

_____ Maria Dworzecka, Department Chair

_____ Peggy Agouris, Dean, The College of Science

Date: _____ Spring Semester 2016
George Mason University
Fairfax, VA

Statistical Modelling of Earth's plasmasphere

A dissertation submitted in partial fulfillment of the requirements for the degree of Doctor of Philosophy at George Mason University

By

Victoir Veibell
Master of Science
George Mason University, 2014
Bachelor of Science
Embry Riddle Aeronautical University, 2010

Director: Robert Weigel, Professor
Department of Department of Computational and Data Sciences

Spring Semester 2016
George Mason University
Fairfax, VA

Dedication

I dedicate this dissertation to ... I dedicate this dissertation to ... I dedicate this dissertation to ... I dedicate this dissertation to ... I dedicate this dissertation to ... I dedicate this dissertation to ... I dedicate this dissertation to ...

Acknowledgments

I would like to thank the following people who made this possible ... I would like to thank the following people who made this possible ...

Table of Contents

List of Tables

Table Page

List of Figures

Abstract

STATISTICAL MODELLING OF EARTH'S PLASMASPHERE

Victoir Veibell, PhD

George Mason University, 2016

Dissertation Director: Robert Weigel

This dissertation intends to first: be a survey of current forecasting capabilities of statistical and magnetohydrodynamic (MHD) methods of Earth's magnetosphere, and second: attempt to improve upon forecasting methods by investigating the usefulness of various new models on both real and modeled data. The forecasting will be separated into two parts: that focusing on rare, but significant events (e.g. geomagnetic storms), and that focusing on general day-to-day predictions. It will encompass three main methods of forecasting: impulse response functions (IRF), nonlinear methods, and statistical methods that attempt to forecast MHD.

Chapter 1: Introduction

1.1 Background

1.1.1 Magnetosphere

Discovery

The dynamic processes of Earth's magnetosphere and their various impacts on the planet and its inhabitants have been studied for centuries: from Celsius and Hiorter who noted a correlation between compass orientation and aurora [1], and the Carrington event in 1859 established the connection between solar output and electromagnetic effects on Earth [2].

It wasn't until Van Allen did his rocket sounding and satellite measurements of high altitude cosmic rays, finding the eponymous Van Allen Radiation Belt, that the structure of the magnetosphere was generally accepted to be more complex than that of a basic dipole magnet [3]. Showing that charged particles in solar wind plasma could be broken into constituent parts and directed into currents led to a deeper understanding of the behavior the magnetosphere and its interconnectivity with structures both inwards and outwards, which in turn allowed for better forecasting of ground-based effects based on solar wind conditions.

Our current computational technology, combined with over 50 years' worth of satellite and ground based measurements [4], allows for a much stronger statistics-based forecasting method to be performed and long-term analyses of the capabilities of computationally intensive forecasting methods.

Processes

The complex structure of the magnetosphere and plasmasphere lead to a number of distinct behaviors and processes such as ring currents, geomagnetic storms, and magnetospheric substorms.

Ring Current The Ring Current, shown in Figure 1.1 is a formed when the magnetosphere splits the neutral solar wind into positive and negative components, where they circle the earth moving along magnetic field lines until they either connect with particles in the upper atmosphere/ionosphere and fall out, or remain trapped in the magnetosphere and slowly drift in opposing directions around the magnetic equator. With enough energetic particles drifting together, a current is generated that can significantly affect the Earth's magnetic field and is labeled the ring current. These particles in the current are injected into the magnetosphere via conditions that cause the solar wind's magnetic field to connect with that of Earth, which is often exacerbated by the surge of energy created by geomagnetic storms.

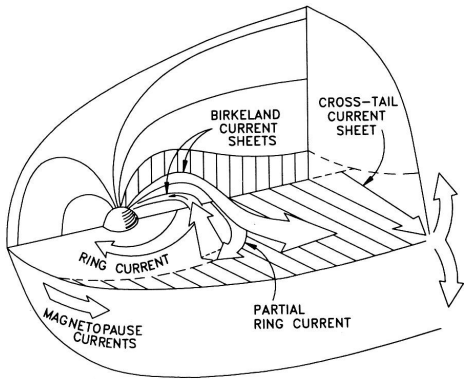

Figure 1.1: Currents in/around the magnetosphere [5]

Geomagnetic storms occur when the solar wind interacts with the Earth's magnetosphere in such a way as to produce significant disruptions in its normal, quiet-time, behavior. It is generally defined by a significant change to the magnetic field measured by multiple ground-based magnetometer measurements from stations spread around the world, in the case of the K_P index, or around the geomagnetic equator in the case of the disturbance storm-time

(D_{st}) index. By using these indices, storms can be classified into categories of severity [6]. The definition of storms in the literature varies slightly between authors [7], but most agree that sustained and abnormally perturbed near-earth magnetic field strengths over several hours or more constitutes a geomagnetic storm [8].

Geomagnetic substorms, in contrast with storms, are much shorter; typically only existing for an hour or two, and potentially happening soon after one another. They tend to have a less appreciable effect on the amount of particles/energy in the ring current, and are associated with sudden changes in energy coming from the tail of the magnetosphere rather than the dayside reconnections associated with storms, and is often directly injected into the polar regions.

Geomagnetic storms and substorms can have significant impacts on Earth and space systems, from inducing currents in large power grids to harming satellite circuitry and onboard data [9]. Because of the potential damage of such events, any ability to forecast a storm could allow operators to prevent or mitigate problems in their systems. Because of the large correlation of CMEs with geomagnetic storms [7], it can be estimated that our forewarning time is the difference between observing a CME (via visual or X-ray methods) and its propagation time plus magnetospheric interaction time. This time can be anywhere from one to five days, depending on the speed of the CME and how it interacts with the interplanetary medium [10]. With a light delay of only eight minutes, this is ample time to see a storm approaching Earth and for operators to react, but a problem lies in the fact that storms are poorly predicted with such lead times [11]. Some storms have slow onsets, some spike suddenly; some have high velocities, and some coincide with large amounts of high-energy particles; no single factor has yet proven to be a good predictor for storms, and while prediction has gradually improved over the years, there remains room for further study.

All of these processes tend to couple earthwards with the plasmasphere, by transferring plasma and radiation from the interplanetary medium down into the Earth's magnetic influence.

1.1.2 Plasmasphere

Discovery

The plasmasphere was largely unknown until the beginning of the space age, being found both through analyses of very low frequency radio waves and in-situ spacecraft measurements. Previously it was believed that electron density decreased continuously from the ionosphere to the interplanetary medium. These experiments showed that the Earth had an envelope of cold plasma around it that ended in an abrupt boundary, and varied in location and density gradient with geomagnetic activity [12].

Processes

The plasmasphere is interconnected with the rest of the magnetosphere, the radiation belts, and the ionosphere. While many of the specifics of this interaction are still not fully understood, some parts have been observed and explained to a reliable degree of accuracy.

At the lowest level, photoionization of oxygen in the ionosphere produces excess electrons that get transferred up into the plasmasphere along magnetic field lines bringing energy/heat along with it. There is also an upward daily "refilling" flux until a saturation point is reached, bringing the lower bounds of the plasmasphere into equilibrium with the upper ionosphere. This flux also typically reverses on the night side, sending electrons back down into the ionosphere.

During periods where the location of the plasmapause is quickly brought earthwards, or a new plasmapause is established, plasma caught outside the plasmapause is known to be magnetically convected outwards and sunwards[13], termed "eroding".

At times, the plasmasphere because distorted at the plasmapause due to dayside reconnection, causing bulges that can become elongated and detached during co-rotation, usually across the dusk side. These extended segments of plasma are known as "plumes" and show up as a peak in density in a normally empty plasmatrough. These plumes also often occur with, and possible because of, enhanced magnetospheric activity[14].

Leave off with list of things that are not well understood and how work in

thesis approaches them.

1.1.3 Radiation Belts

Discovery

The radiation belts that surround Earth, known as the Van Allen Radiation Belts, are two (occasionally three[15]) bands of energetic particles encircling the planet. The existence of such bands was theorized based on knowledge of magnetically trapped motion, and results from rocket soundings that found more radiation in the auroral regions than at the equator. The beginning of the space age allowed particle counters to be sent up on Explorer 1 and Explorer 3, finding radiation far beyond what was anticipated, but concentrated into bands of high density[3].

Processes

The outer radiation belt is filled with particles (mostly electrons) pulled from the solar wind and trapped by the magnetosphere, and occasionally lost when the magnetopause moves back inward. The inner belt tends to be filled by heavier particles (electrons and protons) coming up from the ionosphere, and is overall less variable than the outer belt[15]. The slot region between the two is formed by the interaction of energetic particles with very low frequency (VLF) waves, leading to particle loss to the atmosphere[16].

The various forms of particle movement are shown in Figure 1.2. The primary components being the drift motion leading to the ring current, and the bounce motion leading to the existence of belts of radiation. As particles approach the "Mirror point", a slight angle between the motion and the curvature of the magnetic field line lead to a force opposing the motion along the line, eventually mirroring the particle back in the direction it came from. Since this applies to all particles within a certain range of energies and pitch angles, the collective sum of trapped particles forms the radiation belts.

The azimuthal (equatorial) drift of ions in the radiation belts is what leads to the ring

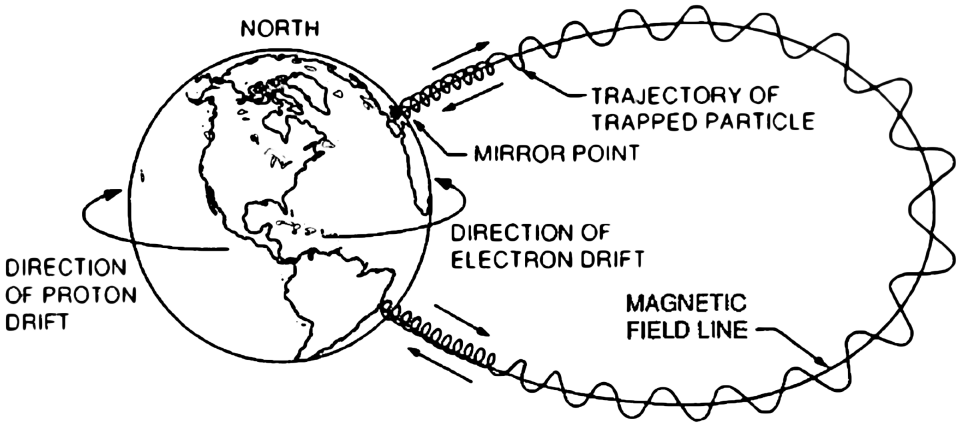

Figure 1.2: Motion of magnetically trapped particles [17]

current. When increased geomagnetic activity causes a change in particles in the radiation belts, this leads to a change in the ring current, which perturbs the Earth's magnetic field noticeably. This perturbation is the basis for the D_{st} index used to gauge magnetic activity.

The radiation belts also have an impact on the plasmasphere by acting as an occasional source of low energy particles and a sink for high energy particles. The plasmasphere also acts on the radiation belts via the VLF waves, energizing electrons out of the plasmasphere and into the radiation belts, or providing particles already in the belts the energy needed to become untrapped[15]. While the outer limits of the plasmasphere and the outer radiation belt often coincide and react similarly to geomagnetic activity, they can become separated during geomagnetically active times [15]. An example of this variation in relative position is shown in Figure 1.3.

denton paper for plasmasphere bounce motion and density along field line correlation with plasmasphere? Mention radiation belt in ring current section and how they're independent. all lowercase)

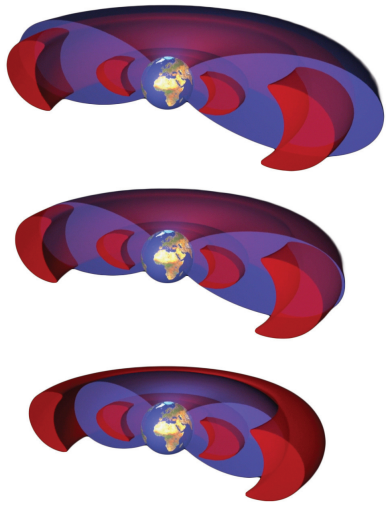

Figure 1.3: Relative position of plasmasphere (blue) and radiation belts (red) with varying geomagnetic activity levels (Adapted from [18].)

1.1.4 Statistical Modeling of Magnetosphere and Plasmasphere

Initial forecasts were based on an observed time delay between sunspots and geomagnetic storms [19]. It then advanced to a basic theory involving electromagnetic interactions in the magnetosphere [20]. There now exist entire services dedicated to executing MHD-based models of the magnetosphere [21], as well as multi-year, multi-institution efforts to survey the general statistics of modeling and forecasting of extreme events [22].

The convergence of the advancement in both statistical and MHD-based simulation has led to a situation where the scientific community has the capacity for monitoring space weather in real time, and forecasting the near-Earth effects. There have been efforts to test the forecast performance of select models over a small number of geomagnetic events [7, 23–25]. However no research has been done that involves the analysis of long-term forecasting performance of these models and comparison of the results with existing methods.

Models specific to the plasmasphere and plasmatrough include Carpenter and Anderson's ISEE/Whistler Model of Equatorial Electron Density in the Magnetosphere, which empirically derives the location and density of the plasmasphere and plasmatrough. They state that the inner edge of the plasmapause is located at $L_{ppi} = 5.6 - 0.46K_{p_{max}}$, with $K_{p_{max}}$ as

the maximum value of K_p in the previous 24 hours. This specifies the outer boundary of the plasmasphere, and from there the density is defined inwards as $n_e = n_{e_{L_{ppi}}} * 10^{-(L-L_{ppi})/\Delta pp}$, where $n_{e_{L_{ppi}}}$ relates day number, sunspot number, whistler profiles, and multiple year long perturbations in an exponential fashion shown as $n_e(L, d, \bar{R}) = 10^{\Sigma x_i}$. L_{ppi} and Δpp are empirically derived plasmapause location and width, respectively.

Gallagher and Craven's Global Core Plasma Model [26], which empirically links plasma density and magnetosphere conditions by fitting Carpenter's equation but includes a sinusoidal dependence on magnetic local time (MLT) with the other considerations for density. At the most basic level, it reduces to an exponential equation of the form $n_{ps} = 10^{gh} - 1$, where g and h are terms relating to the inner plasmasphere and plasmapause, but the derivations of g and h are where the complexities of the model come into play.

Moldwin [27] builds on this model by refining the empirically derived plasmapause location with new measurements and an in-depth analysis of the bounds of the previously established models.

O'Brien [28] finds that using auroral electrojet (AE) or disturbance storm time (D_{st}) indices work better than KP for determining plasmapause location.

Theoretical models of plasmasphere (CIMI?), comparison to empirical measurements (CLUSTER, IMAGE, THEMIS). Tie in with results. Discuss current results based on plasmapause but current study focused on plasmatrough (Denton and Takahashi show most data in plasmatrough)

Make connection to each paper with a section in chapter 2.

Chapter 2: Methods

This work utilized a number of linear and nonlinear methods of analysis and modeling, including Auto-Regressive Moving Average models with eXogenous inputs (ARMAX) and neural net models. No single method is ideal, and using many methods is better for insight, especially for nonlinear/complex systems. The details of their application will be expanded upon in their respective sections.

2.1 Linear

2.1.1 Overview

Due to its simplicity and ease of application, linear models are used in practically all fields as a first attempt to discover information about the data and any potential relationships. In Space Physics, where the underlying behavior of a complex system is not theoretically known, and in-situ measurements are sparse, linear models are often the first step towards understanding what components are related and to what degree. Sometimes this leads to understanding unexpected complexities in a system. **Example. Lemaire p.183 heavier ions in outer plasmasphere than inner plasmasphere? Correlation between plasmapause and radiation belt boundary?**

2.1.2 ARX

Impulse response systems are systems in which the output (a response) is driven by a linear sum of coefficients of an input (a series of impulses). A simple example would be making a loud noise in a concert hall. The response will be the unique echoes and reverberations

created by the initial driving sound, and with enough signal, a statistical model can be generated that will map the input sound to a response echo. In the magnetosphere, the most used example is an impulse of v_{B_s} driving the Auroral Electrojet (AE/AL) index [29], or the Disturbance Storm Time (D_{st}) index [30], also shown in Figure 2.1.

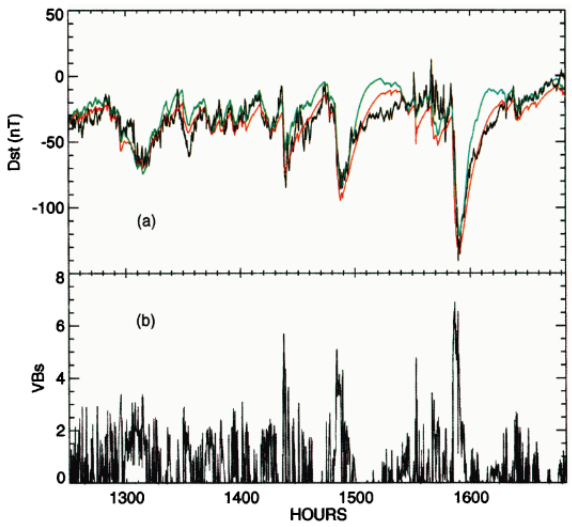

Figure 2.1: DST (black), nonlinear autoregressive exogenous (ARX) model (red), Burton et al 1975 model (green). (b) v_{B_S} impulse as input.[31]

Convert figures to eps

This plot shows how different models are used to predict magnetospheric variables with varying amounts of success. In this proposal, what starts as a simple Box-Jenkins model of the form [32]:

$$x(t) = c + \sum_{j=0}^{m} a_j f(t - j\Delta t)$$

can be modfied with an auto-regressive component to be an autoregressive model with exogenous inputs (ARX) such as that used in [31], taking the form:

$$\hat{x}(t + \Delta t) = \sum_{i=0}^{l} a_i \cdot x(t - i\Delta t) + \sum_{j=0}^{m} b_j \cdot f(t - j\Delta t) + c \tag{2.1}$$

Where m and l are the number of coefficients desired for including previous data points in the prediction, and c is a factor to remove the mean offset from the data. Note that in some cases the starting value of the iterators can be individually increased if there is a known delay in response time or there is a desire to predict further into the future. In [31], second order equations ($m = 2$) were used with anywhere from one to four driving coefficients, but in practice any number of coefficients and any number of driving variables can be used up to some fraction of the number of data points that allows the coefficient matrices to be solved for.

There generally is a limit to the usefulness of large-lag data [22]. By looking at a plot of the cross correlation relative to the number of coefficients, a limit will generally be seen where adding more coefficients no longer reduces error in the model. By creating a threshhold of change in fit per coefficient added (perhaps via a bootstrap method), the minimum number of coefficients needed to optimally model the system can be determined.

By constructing a linear system of equations from Equation 2.1, the coefficients can be solved for in a general matrix form (where, in this case, $l = m$):

$$\begin{pmatrix} x_0 & ... & x_{l-1} & f_0 & ... & f_{l-1} & 1 \\ x_1 & & x_l & f_l & & f_l & 1 \\ ... & & & & & & \\ x_{N-l} & ... & x_{N-1} & f_{N-l} & ... & f_{N-1} & 1 \end{pmatrix} \begin{pmatrix} a_0 \\ ... \\ a_{l-1} \\ b_0 \\ ... \\ b_{l-1} \\ c \end{pmatrix} = \begin{pmatrix} x_l \\ x_{l+1} \\ ... \\ x_N \end{pmatrix}$$

This is a linear model for the behavior of a system. However, it has been shown that the set of coefficients describing the response of a system can change with storm intensity [31], the time scale modeled [33], and even the time of day [29]. This creates a very large number of possible directions for research, from predicting storm onsets, to predicting storm

intensities, to modeling the overall shape and behavior of a storm, as well as all of the other possible interactions outside of storm-time.

2.1.3 ARMAX

A class of model known as an Auto-Regressive Moving Average with eXogenous inputs model (ARMAX) is often used in time series analysis to combine the effects of persistence, linear dependence, and an average that changes with time. It makes a slight change on the ARX model in Equation 2.1, adding the moving average term:

$$\hat{x}(t+\Delta t) = \sum_{i=0}^{l} a_i \cdot x(t-i\Delta t) + \sum_{j=0}^{m} b_j \cdot f(t-j\Delta t) + \sum_{k=0}^{n} c_k \cdot g(t-k\Delta t) + c_{t+\Delta t} \quad (2.2)$$

Clean up notation (c_t or c_n? All go 0 to t?)

2.1.4 Applicability

As implied by the name, an ARMAX model is suitable for analysis of a time-dependent linear system where the value of a measurement is determined by its own persistence, an external variable, and some factor that contributes to a moving average with time. Most linear systems can be encapsulated by this framework, some even being overspecified with this level of accounting for variability.

2.1.5 Caveats and Biases

There will be a number of things that, ideally, must come together to make this kind of data prediction work. For one: ARX methods can often be heavily dependent on a concept known as "persistence", whereby the best prediction for a variable at any time is that same variable at the last measured time step. For example, if the high temperature today is 70°, it is fairly likely that the high temperature tomorrow will be near 70°. Too much reliance on persistence forecasting, though, and predictions can lose their usefulness. Figure

2.2, for example, shows how a model can achieve high correlation with persistence, but be almost entirely useless for predicting events before they happen since the spikes are never anticipated, just modeled after they've already been seen.

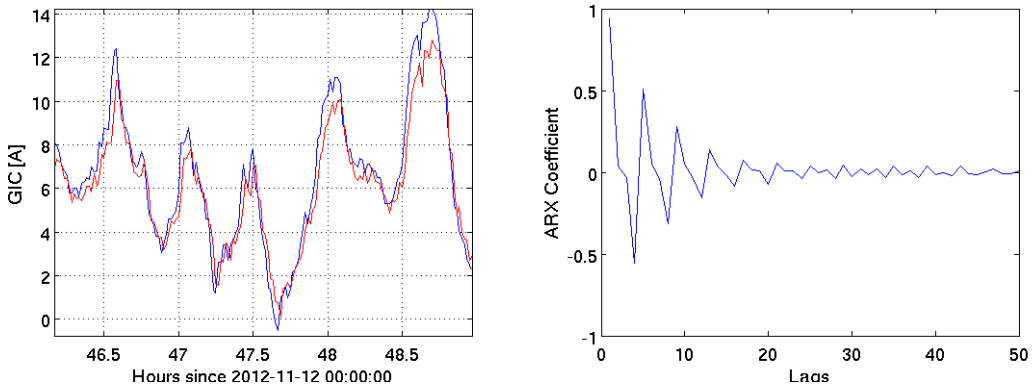

Figure 2.2: Persistence forecast; model in red

In this case, it is clear that the largest auto-correlation coefficient comes at 1 time lag, meaning the most recent measurement has the most weight in a forecast. For day-to-day behavior, this is acceptable as being part of the behavior of the system. For the forecasting of extreme events, however, another metric must be used that measures the ability of the model to predict events at or before their actual occurrence, while simultaneously avoiding predicting events that do not happen. One method for comparing models in this fashion is by using the Heidke Skill Score [34, 35], which is based on the quantity:

$$S = \frac{R - E}{T - E}$$

where R is the number of correct forecasts, T is the total number of forecasts, and E is the number expected to be correct by, in this case, a persistence forecast. This can be adapted to either consider a range of "correctness", or a binary threshold to be met. It may also be desired to assign a cost-weighting to success rates. If, say, it costs $1 million to prepare a power grid for a storm, 10 false alarms to every one storm gets costly unless successfully preparing for that one storm saves $1 billion. To do this, a measure of the utility of a

forecast can be quantified [11]:

$$U_F \equiv BN_H - CN_{\bar{H}} > 0$$

Where N_H is the number of correct forecasts, $N_{\bar{H}}$ is the number of false alarms, C is the cost of taking mitigating action, and B is the benefit from correctly taking mitigating action. This method has caveats discussed in [11], but is a useful metric for forecast utility when costs are known, and some measure of success can be determined.

The other major problem in forecasting is that of lead time. Being able to forecast a storm one minute in advance is generally not enough time for operators to take mitigating action.

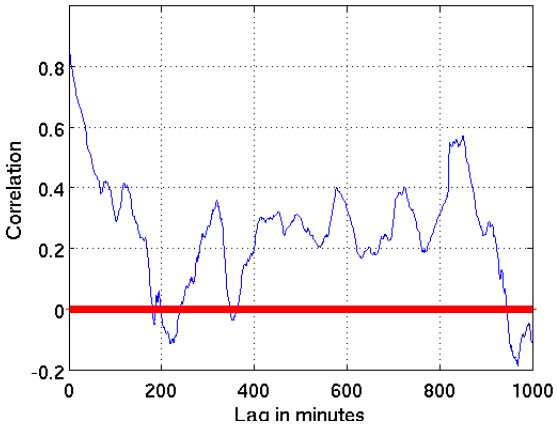

Figure 2.3: Correlation vs lags

Figure 2.3 shows a set of predictions made for autocorrelation in geomagnetically-induced currents (GIC). This metric is a measure of how much electric currents in the magnetosphere induce currents in ground-based electrical systems. The predictions were made further and further in time from the current magnetic field and GIC measurements, with decreasing accuracy as the predicted time got further from the current time. While an accurate prediction can be made one minute in advance, a prediction 3 hours in advance has almost no correlation with what actually happens. This is the main problem that this dissertation hopes to address.

Mean vs Median

The question of whether to use means or medians for analysis is based on what facets of the data are most important to the research. Since means biased towards outliers and medians biased against them, the decision rests on how much weight should be given to outliers (or extreme values) in a study. For example, when looking at long-term solar wind variables, intermittent spikes may not be relevant to the overall pattern of behavior being analyzed, but knowing that on a short time scale a certain day had a noticeable spike may be important. In the former case, using the median would likely be best, and using the mean for the latter. However, space physics often deals with skewed distributions and sparse data, leading to an uncertainty of which method is best, so both are and analyzed with their respective traits in mind. **Numerically specific result**

Effects of time averaging

Similarly to the mean vs median question, the decision on if/how much to average the data over time will affect the resulting time series to be biased against intermittent spikes in value. The more time added to any particular average, the less impact any short-term changes will have on the final value.

2.1.6 Summary

reitterate relevance

2.2 Nonlinear

2.2.1 Overview

Other models were used to test nonlinear approaches to forecasting. The first choice was a model based on neural networks [23, 36] which approximates a non-linear system given a

set of training data. The usefulness of this is apparent in a few key points: the weights of contribution of any particular variable to a system will likely be nonlinear in some fashion (e.g. a ground station's measurements will depend on sunlight heating the ionosphere which depends on latitude, time of year, and time of day), and allowing for the non-linear effects of saturation where perhaps the magnetosphere will behave differently after reaching certain levels of particle density or electric potential, rather than directly scaling regardless of limits.

Another algorithm known as Principal Component Analysis (PCA) can be used to take the large number of possible variables and define an orthogonal set of vectors that most efficiently encapsulate the variance in the data. By doing this, the number of variables needed for computing any linear or non-linear algorithm can be reduced and optimized, making predictions quicker while maintaining most of the predictive benefits of using all possible data.

2.2.2 Neural Networks

2.2.3 Applicability

Nonlinear models are applicable when a system has more complexity than can be encapsulated by a linear model. Since they're usually a class of model that trains adaptive weights that can be tuned by known inputs and outputs, they're especially useful for systems where a large amount of training data are available.

2.2.4 Caveats and Biases

Nonlinear models can be susceptible to overfitting, since they inherently attempt to fit more complexity than a linear model, but can also be controlled via the number of inputs and weights used. They also may suggest more structure than might truly exist. Both of these problems are lessened by training with more data, if available. Figure 2.4 shows a comparison of predicting equatorial mass density (ρ_{eq}) with the $F_{10.7}$ index and solar wind velocity (V_{sw}). The neural net model shows much more structure than the linear model despite being given the same data. Whether that structure reflects any real physical

phenomenon, however, is a difficult problem to answer.

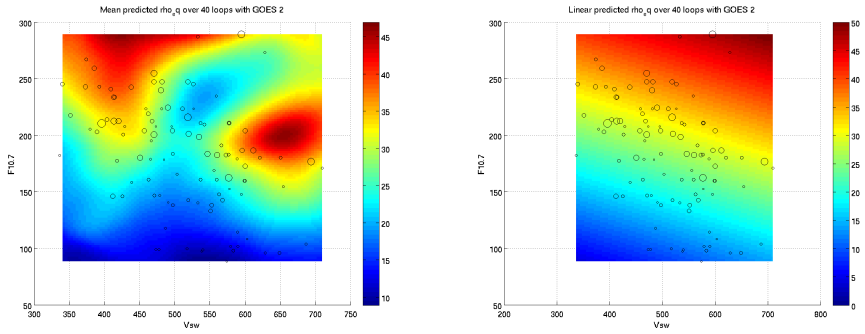

Figure 2.4: Nonlinear model vs linear model of ρ_{eq}

2.2.5 Comparison to Linear Model

Nonlinear models differ from linear models by incorporating some method for accounting for effects within a domain that are not seen across the entire domain. Though both models can be given the same inputs, and trained on the same outputs, the models themselves can fundamentally differ. Linear models are also generally simple to interpret (e.g. $y = 2 * x$ means for every change in x, y changes by double that amount.) Nonlinear models, on the other hand, generally have no simple interpretation and must be approached by testing for a range of parameters in the model to map out resulting outputs and make some interpretation of the underlying structure.

2.2.6 Summary

Results nonlinear

Note that you always compare performance relative to linear model as a reference point. Useful for determining how important nonlinearity is.

Appendix A: An Appendix

This is an appendix. Here is a numbered appendix equation:

$$a^2 + b^2 = c^2. \tag{A.1}$$

Bibliography

[1] W. Soon and S. H. Yaskell, *The Maunder Minimum and the Variable Sun-earth Connection*. World Scientific, 2003.

[2] R. C. Carrington, "Description of a Singular Appearance seen in the Sun on September 1, 1859," *Monthly Notices of the Royal Astronomical Society*, vol. 20, pp. 13–15, Nov. 1859.

[3] H. Newell, *Beyond the Atmosphere Early Years of Space Science*. City: Dover Publications, 2011. [Online]. Available: http://history.nasa.gov/SP-4211/contents.htm

[4] R. Snare, "A History of Vector Magnetometery in Space." [Online]. Available: http://www-ssc.igpp.ucla.edu/personnel/russell/ESS265/History.html

[5] D. P. Stern, "The art of mapping the magnetosphere," *Journal of Geophysical Research: Space Physics*, vol. 99, no. A9, pp. 17 169–17 198, 1994. [Online]. Available: http://dx.doi.org/10.1029/94JA01239

[6] N. Oceanic and A. Administration, "NOAA Space Weather Scales," 2005. [Online]. Available: http://www.swpc.noaa.gov/NOAAscales/

[7] Y. I. Yermolaev and M. Y. Yermolaev, "Statistic study on the geomagnetic storm effectiveness of solar and interplanetary events," *Advances in Space Research*, vol. 37, pp. 1175–1181, 2006.

[8] J. T. Gosling, D. J. McComas, J. L. Phillips, and S. J. Bame, "Geomagnetic activity associated with earth passage of interplanetary shock disturbances and coronal mass ejections," *Journal Of Geophysical Research*, vol. 96, pp. 7831–7839, May 1991.

[9] J. Allen, L. Frank, H. Sauer, and P. Reiff, "Effects of the March 1989 solar activity," *EOS Transactions*, vol. 70, p. 1479, Nov. 1989.

[10] J. Zhang, I. G. Richardson, D. F. Webb, N. Gopalswamy, E. Huttunen, J. C. Kasper, N. V. Nitta, W. Poomvises, B. J. Thompson, C.-C. Wu, S. Yashiro, and A. N. Zhukov, "Solar and interplanetary sources of major geomagnetic storms (Dst $\leq$ -100 nT) during 1996-2005," *Journal of Geophysical Research (Space Physics)*, vol. 112, p. 10102, Oct. 2007.

[11] R. S. Weigel, T. Detman, E. J. Rigler, and D. N. Baker, "Decision theory and the analysis of rare event space weather forecasts," *Space Weather*, vol. 4, p. 5002, May 2006.

[12] J. Lemaire, *The earth's plasmasphere*. Cambridge, U.K. New York: Cambridge University Press, 1998.

[13] D. L. Carpenter and J. Lemaire, "Erosion and Recovery of the Plasmasphere in the Plasmapause Region," *Space Science Reviews*, vol. 80, pp. 153–179, Apr. 1997.

[14] R. C. Elphic, L. A. Weiss, M. F. Thomsen, D. J. McComas, and M. B. Moldwin, "Evolution of plasmaspheric ions at geosynchronous orbit during times of high geomagnetic activity," *Geophysical Research Letters*, vol. 23, pp. 2189–2192, 1996.

[15] F. Darrouzet, V. Pierrard, S. Benck, G. Lointier, J. Cabrera, K. Borremans, N. Y. Ganushkina, and J. D. Keyser, "Links between the plasmapause and the radiation belt boundaries as observed by the instruments CIS, RAPID, and WHISPER onboard Cluster," *Journal of Geophysical Research (Space Physics)*, vol. 118, pp. 4176–4188, Jul. 2013.

[16] S. F. Fung, X. Shao, and L. C. Tan, "Long-term variations of the electron slot region and global radiation belt structure," Geophys. Res. Lett., vol. 33, p. L04105, Feb. 2006.

[17] M. Walt, *Introduction to geomagnetically trapped radiation*. Cambridge New York: Cambridge University Press, 1994.

[18] C. Carreau, "Earth's plasmasphere and the van allen belts." [Online]. Available: http://sci.esa.int/cluster/52831-earth-plasmasphere-and-the-van-allen-belts/

[19] R. S. Richardson, "Sun-Spots and Magnetic Storms," *Leaflet of the Astronomical Society of the Pacific*, vol. 2, p. 133, 1936.

[20] S. Chapman and V. C. A. Ferraro, "A new theory of magnetic storms," *Terrestrial Magnetism and Atmospheric Electricity (Journal of Geophysical Research)*, vol. 36, p. 77, 1931.

[21] CCMC, "Community coordinated modeling center." [Online]. Available: http://ccmc.gsfc.nasa.gov/

[22] M. Ghil, P. Yiou, S. Hallegatte, B. D. Malamud, P. Naveau, A. Soloviev, P. Friederichs, V. Keilis-Borok, D. Kondrashov, V. Kossobokov, O. Mestre, C. Nicolis, H. W. Rust, P. Shebalin, M. Vrac, A. Witt, and I. Zaliapin, "Extreme events: dynamics, statistics and prediction," *Nonlinear Processes in Geophysics*, vol. 18, pp. 295–350, May 2011.

[23] R. Bala and P. Reiff, "Improvements in short-term forecasting of geomagnetic activity," *Space Weather*, vol. 10, p. 6001, Jun. 2012.

[24] N. A. Tsyganenko and M. I. Sitnov, "Modeling the dynamics of the inner magnetosphere during strong geomagnetic storms," *Journal of Geophysical Research (Space Physics)*, vol. 110, p. 3208, Mar. 2005.

[25] J. Zhang, M. W. Liemohn, J. U. Kozyra, M. F. Thomsen, H. A. Elliott, and J. M. Weygand, "A statistical comparison of solar wind sources of moderate and intense geomagnetic storms at solar minimum and maximum," *Journal of Geophysical Research (Space Physics)*, vol. 111, p. 1104, Jan. 2006.

[26] D. L. Gallagher, P. D. Craven, and R. H. Comfort, "Global core plasma model," J. Geophys. Res., vol. 105, p. 18, Aug. 2000.

[27] M. B. Moldwin, L. Downward, H. K. Rassoul, R. Amin, and R. R. Anderson, "A new model of the location of the plasmapause: CRRES results," *Journal of Geophysical Research (Space Physics)*, vol. 107, p. 1339, Nov. 2002.

[28] T. P. O'Brien and M. B. Moldwin, "Empirical plasmapause models from magnetic indices," Geophys. Res. Lett., vol. 30, pp. 1–1, Feb. 2003.

[29] L. F. Bargatze, D. N. Baker, E. W. Hones, Jr., and R. L. McPherron, "Magnetospheric impulse response for many levels of geomagnetic activity," *Journal of Geophysical Research*, vol. 90, pp. 6387–6394, Jul. 1985.

[30] C. R. Clauer, R. L. McPherron, C. Searls, and M. G. Kivelson, "Solar wind control of auroral zone geomagnetic activity," *Geophysical Research Letters*, vol. 8, pp. 915–918, Aug. 1981.

[31] A. J. Klimas, D. Vassiliadis, and D. N. Baker, "Dst index prediction using data-derived analogues of the magnetospheric dynamics," *Journal of Geophysical Research*, vol. 103, pp. 20 435–20 448, Sep. 1998.

[32] R. S. Weigel, "Solar wind time history contribution to the day-of-year variation in geomagnetic activity," *Journal of Geophysical Research (Space Physics)*, vol. 112, p. 10207, Oct. 2007.

[33] D. Vassiliadis, R. S. Weigel, D. N. Baker, S. G. Kanekal, and A. J. Klimas, "Probing the solar wind-inner magnetospheric coupling: validation of relativistic electron flux models," *Journal of Atmospheric and Solar-Terrestrial Physics*, vol. 66, pp. 1399–1409, Oct. 2004.

[34] P. Heidke, "Berechnung des Erfolges und der Güte der Windstärkevorhersagen im Sturmwarnungsdienst," *Geografiska Annaler*, vol. 8, pp. 310–349, 1926. [Online]. Available: http://www.jstor.org/stable/519729?seq=4

[35] G. Brier and R. Allen, "Verification of Weather Forecasts," *Compendium of Meteorology*, pp. 841–848, 1951. [Online]. Available: http://archive.org/stream/compendiumofmete00amer#page/840/mode/2up

[36] J. V. Hernandez, T. Tajima, and W. Horton, "Neural net forecasting for geomagnetic activity," *Geophysical Research Letters*, vol. 20, pp. 2707–2710, Dec. 1993.

Curriculum Vitae

Include your *curriculum vitae* here detailing your background, education, and professional experience.